Spontaneously gapped ground state in suspended bilayer graphene

F. Freitag,[1] J. Trbovic,[1] M. Weiss,[1] and C. Schönenberger[1,*]

[1]*Department of Physics, University of Basel, Klingelbergstrasse 82, CH-4056 Basel, Switzerland*

(Dated: January 20, 2013)

Bilayer graphene bears an eight-fold degeneracy due to spin, valley and layer symmetry, allowing for a wealth of broken symmetry states induced by magnetic or electric fields, by strain, or even spontaneously by interaction. We study the electrical transport in clean current annealed suspended bilayer graphene. We find two kind of devices. In bilayers of type B1 the eight-fold zero-energy Landau level (LL) is partially lifted above a threshold field revealing an insulating $\nu = 0$ quantum Hall state at the charge neutrality point (CNP). In bilayers of type B2 the LL lifting is full and a gap appears in the differential conductance even at zero magnetic field, suggesting an insulating spontaneously broken symmetry state. Unlike B1, the minimum conductance in B2 is not exponentially suppressed, but remains finite with a value $G \lesssim e^2/h$ even in a large magnetic field. We suggest that this phase of B2 is insulating in the bulk and bound by compressible edge states.

PACS numbers: 72.80.Vp, 73.43.Qt, 73.23.-b, 73.22.Pr, 73.22.Gk

Two dimensional electron systems (2DES) can host a large variety of ground states. Celebrated examples are the fractional quantum-Hall effect [1–3] and the Wigner crystal [4], both being driven by Coulomb interaction. Bilayer graphene provides a further class of interacting 2DES [5]. In contrast to single layer graphene, the chiral charge carriers are massive due to the coupling between the two layers [6, 7]. Owing to the large number of symmetries, a wealth of ground states has been predicted [8–13].

Bilayer graphene proves to be interesting in terms of electron-electron interaction. In comparison with single layer graphene the interaction parameter r_s is about 30 times higher and proportional to $1/\sqrt{n}$, where n is the charge carrier density [5]. The Coulomb interaction can even further be increased by suspending the sample. Furthermore, cleaner devices can be obtained by current annealing [14, 15]. The subsequently lower disorder potential enables one to reach a lower minimal carrier concentration n at the charge neutrality point (CNP). At and around the CNP, electron-electron interaction has been predicted to be able to spontaneously open a gap [8–13]. This is opposed to an induced gap from the application of an external field [16–18] or mechanical strain [19, 20].

Bilayer graphene has an eightfold degenerate LL at zero energy. As the Hall conductivity is quantized at values of $\sigma_{xy} = \nu \cdot e^2/h$, where the filling factor ν is given by $\nu = \pm 4(N+1)$, a step of $8e^2/h$ is observed from $\nu = -4$ to $\nu = 4$ around the CNP [7]. The eightfold zero-energy LL degeneracy can be lifted. For example, the Zeeman energy is able to break the spin symmetry. This manifests itself in a partial lifting with a quantum Hall plateau appearing at $\nu = 0$ [21]. A breaking of symmetries can also be induced by strong electron-electron interaction [12, 22]. If all symmetries are lifted, quantum Hall plateaus appear at filling factors $\nu = 0, \pm 1, \pm 2, \pm 3, \ldots$. Magnetic fields of $30 - 45\,\mathrm{T}$ were required to see this lifting in silicon dioxide supported devices, for both single [23] and bilayer graphene [24], until Feldman *et al.* succeeded in observing the effect at low magnetic fields in suspended bilayer graphene [21].

The most striking state is the $\nu = 0$ state, whose nature is under debate for both single layer [25–27] and bilayer graphene [18, 21, 24]. For bilayer graphene, several possibilities are being discussed, such as the quantum Hall ferromagnet (QHF) [12, 22], the quantum anomalous Hall insulator (AHI) [11, 28], or a ferroelectric phase [10]. Using differential conductance spectroscopy, we find a new class of bilayer samples, which are evidentially gapped at the CNP in zero magnetic and electric field.

Suspended graphene devices were fabricated by mechanical exfoliation of natural graphite transferred to a doped Si wafer with a 300 nm top SiO_2 layer. The number of graphene layers was determined by Raman spectroscopy. The devices were then annealed for several hours in vacuum (10^{-7} mbar) at 200 °C before the electrical contacts made from Cr/Au (1/70 nm) bilayers were fabricated by electron-beam lithography. Thereafter, SiO_2 was etched in buffered hydrofluoric acid (HF). After mounting a device into a ^{3}He cryostat, we performed current annealing by applying a DC current at 1.5 K. This procedure was repeated with higher currents until the electrical conductance $G(V_g)$ as a function of the gate voltage V_g applied to the doped substrate showed a pronounced dependence with a charge neutrality point (CNP), where G has a minimum, close to $V_g = 0$, reminiscent of a high quality device (this usually required current densities of up to $8 \cdot 10^7\,\mathrm{A/cm^2}$). Conductance measurements were carried out with a lock-in amplifier applying a $20\,\mu$V AC voltage onto which a DC bias voltage could be superimposed.

Fig. 1 shows representative measurements of the two-terminal conductance G of suspended graphene devices when n is altered by the back-gate voltage V_g. The CNP is close to $V_g = 0$ V for all samples, indicating that only few charged impurities reside on the graphene. Both sin-

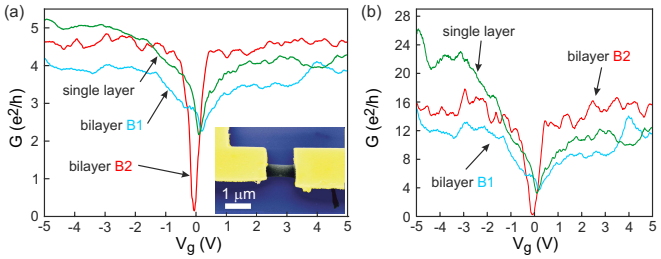

FIG. 1: (Color online) (a) Comparison of the measured dependence of the conductance G on the applied gate voltage V_g for three suspended devices: monolayer graphene (length×width $1{\times}2\ \mu m^2$, $T = 2$ K), bilayer type B1 ($2{\times}0.8\ \mu m^2$, $T = 230$ mK), and bilayer type B2 ($1{\times}1.5\ \mu m^2$, $T = 230$ mK). In (b) the contact resistance has been subtracted.

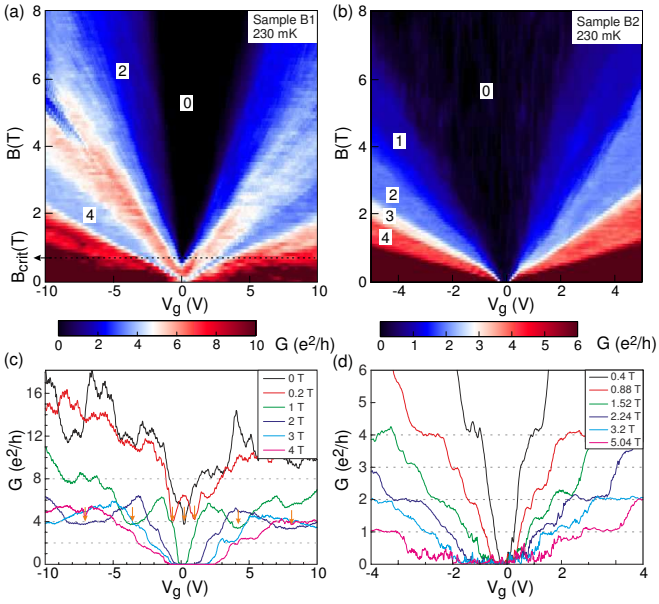

FIG. 2: (Color online) The dependence of the linear conductance G on the gate voltage V_g and perpendicular magnetic field B reveal two type of samples. In sample B1, shown in (a,c) the plateaus at filling factors $\nu = 0$, ±2 and ±4 are well developed. The $\nu = \pm4$ plateau (minima in (c), see arrows) extends to very low magnetic fields. For sample B2, a full lifting of the eightfold Landau level degeneracy is observed, as plateaus at odd fillings appear as well. The curves in (c,d) show lines cuts at constant B. Appropriate contact resistances were subtracted.

gle layer and bilayers of type B1 display a smooth transition from low G at the CNP to higher G values at larger n, as expected from the V-shaped conductances found in recent literature [21, 29, 30]. In contrast, bilayer samples of type B2 are very low conducting at the CNP with $G_{min} < 0.2\ e^2/h$ at 230 mK, which is considerably lower than in previous reports [18]. Furthermore, as the gate voltage is tuned away from the CNP, G increases sharply and then quickly saturates for $|V_g| > 0.5$ V. Note, that this is even the case, when the contact resistance is subtracted as shown in Fig. 1b.

When placed in a perpendicular magnetic field B, samples B1 and B2 reveal substantially different quantum Hall features, as shown in Fig. 2. As the measurements were performed in a two-terminal configuration, they include a contact resistance [31]. We determine the contact resistance by matching G to the closest integer value of the quantized Hall conductance (supplemental material [32]) and then subtracted it from the data. First, we discuss sample B1 and then sample B2.

In sample B1 we observe a partial lifting of the eightfold zero energy LL degeneracy, leading to the $\nu = \pm2$ and 0 states above a critical magnetic field of $B_{crit} \approx 0.75$ T (Fig. 2a). In the magnetic field range $0 \leq B \leq 0.75$ T we observe the same Hall sequence as in conventional devices where the conductance has a step of $8e^2/h$ from $\nu = -4$ to $+4$. When applying $B > B_{crit}$ an insulating state emerges around the CNP, followed by the $\nu = \pm2$ state with a two-fold degeneracy remaining. We also note that the $\nu = \pm4$ state appears to extend all the way down to the CNP at zero magnetic field [11, 33]. The corresponding line cuts from the color scale are shown in Fig. 2c to illustrate the evolution of the CNP into the $\nu = \pm4$ state at low fields and the appearance of the broken symmetry states $\nu = 0$ and ±2 at higher fields [21]. Unlike sample B1, B2 shows a fully lifted zero-energy LL, manifesting in the appearance of Hall plateaus for odd filling factors ν. In analogy to sample B1, we label the low conducting region around the CNP in sample B2 with $\nu = 0$, although this state maintains a finite conductance as we will discuss below.

In the following Fig. 3 we investigate the properties of the low conducting state at $\nu = 0$ at low charge carrier density as a function of B and T for both samples. For device B1 (Fig. 3a), we find that at low B the resistance R at the CNP remains around $R = 6\,\mathrm{k}\Omega$, but when a critical perpendicular magnetic field of $B_{crit} \approx 0.75$ T is reached, it increases sharply to $10^8\,\Omega$, the maximum resistance that our measurement set-up can resolve. This behavior can be attributed to the formation of a quantum Hall state at $\nu = 0$ [26]. Since the Fermi energy now lies in between two Landau levels, a thermally activated behavior is expected for the electrical resistance R. This is confirmed in the experiment, revealing a strong dependence of R on temperature T above the critical field following the law $R \propto exp(\Delta E/2k_BT)$ [32]. The activation energy ΔE is linearly dependent on B with a value that amounts to $1.1\,\mathrm{meV/T} = 13\,\mathrm{K/T}$. Note, that the spin Zeeman splitting is much smaller, only amounting to $\sim 0.7\,\mathrm{K/T}$. Feldman *et al.* [21] deduce in their experiment $\Delta E = 3.5 - 10.5\,\mathrm{K/T}$, which is somewhat lower than our number. In a recent theory, taking interactions into account, the energy gap of the $\nu = 0$ state has been calculated to be $14.3\,\mathrm{K/T}$ [12].

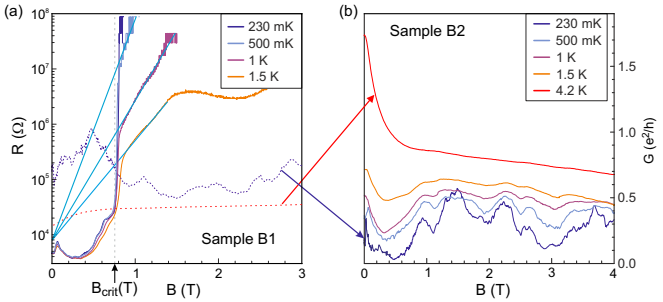

FIG. 3: (Color online) Difference in resistance R (a) of sample B1 and conductance G (b) of sample B2 as a function of magnetic field B at the CNP. A sharp transition to an insulating $\nu = 0$ state appears at $B_{crit} = 0.75\,\mathrm{T}$ (arrow) in B1. In this state, R is thermally activated [32] with an activation energy ΔE proportional to B. The lines are guides to the eyes for this dependence. For comparison we show the resistance data for sample type B2 (dotted) within the same graph. In contrast to sample B1, sample B2 does not show a field-induced transition to an insulating state. At low temperatures, G is remarkably insensitive to B, but displays a relatively low conductance value $< e^2/h$. Appropriate contact resistances are subtracted.

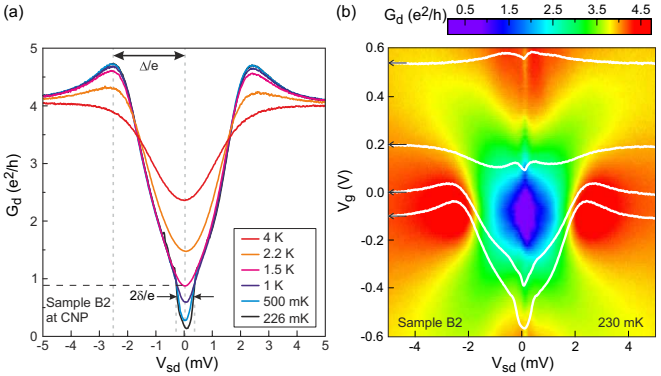

FIG. 4: (Color online) (a) Temperature dependence of the differential conductance G_d around the CNP of sample B2 as a function of the source-drain bias voltage V_{sd}. Two gaps with size $\Delta = 2.5$ meV and $\delta = 0.35$ meV appear that both display a distinct temperature dependence. (b) Color-scale of G_d as a function of V_{sd} and gate voltage V_g at 230 mK. Line cuts are taken at the values of V_g marked by the arrows.

The dotted curves in Fig. 3a show the resistance of B2 in direct comparison to that of B1 at 230 mK and 4 K. We find that at $B = 0\,\mathrm{T}$ B2 has an order of magnitude higher resistance than B1, whereas at higher magnetic fields, B1 is several orders more resistive. Fig. 3b elaborates on the conductance of B2 at the CNP as a function of B and temperature. Most notably, G at $B \gtrsim 1\,\mathrm{T}$ is nearly independent of B with the exception of fluctuations most likely due to localized states [3].

The marked differences in the magnetic field dependence clearly demonstrate that sample B1 and B2 differ. In sample B1, the LL degeneracy is partially lifted for $B > B_{crit} \approx 0.75\,\mathrm{T}$. This lifting includes a transition into a $\nu = 0$ quantum Hall plateau in the vicinity of the CNP. On the other hand, sample B2 reveals a fully lifted LL, where all Hall plateaus appear already a small $B \sim 1\,\mathrm{T}$. Furthermore, sample B2 stays conductive at the CNP even at higher B of up to 8 T. We note, that sample B1 is similar in characteristics to the one reported by Feldman *et al.* [21], whereas B2 shows new features.

We further investigate the nature of sample B2 by measuring the differential conductance G_d as a function of the applied DC bias V_{sd} between source and drain contacts at $B = 0\,\mathrm{T}$ at the CNP ($V_g = -0.1\,\mathrm{V}$), where G_d is suppressed. Fig. 4a summarizes the findings for different temperatures from 226 mK to 4 K (no contact resistance subtracted). Two gaps can clearly be identified: When going from large source-drain bias $V_{sd} > 4\,\mathrm{mV}$ towards small voltages, the larger gap Δ sets in at $V_{sd} = \pm 2.5\,\mathrm{mV}$, where G_d is decreased from around $4e^2/h$ to $0.9e^2/h$ in the data measured at 226 mK. The smaller gap δ appears at voltages $|V_{sd}| \lesssim 0.35\,\mathrm{mV}$ and it reduces G_d from $0.9e^2/h$ to less than $0.2e^2/h$. By increasing the temperature from 226 mK on, the smaller gap δ is first reduced and then vanishes at 1 K.

In order to identify the origin of these two gaps, a color scale plot of the differential conductance G_d against V_{sd} and the gate voltage V_g at 230 mK is shown in Fig. 4b. The line cut at the CNP ($V_g = -0.1\,\mathrm{V}$) shows again the two gaps in electron transport. As V_g and thus the charge carrier concentration is increased, the two gaps exhibit distinct changes. The larger gap Δ disappears, while the smaller gap δ still exists in the metallic graphene regime at $V_g > 0.5\,\mathrm{V}$ but the relative dip is less pronounced. This behavior is qualitatively consistent with Coulomb charging of the whole flake [34]. We estimate a single-electron charging energy of 1 meV for a flake of width 1.5 μm. Because the contact conductances of $\sim 4-8\,e^2/h$ are substantially larger than e^2/h, charge quantization is only weak and no strong Coulomb blockade gap is expected. One rather expects the conductance to display a 'weak' conductance suppression by something like $25-50\,\%$ around zero bias, in agreement with the observation. In contrast to the small gap, the larger gap Δ is strongly dependent on the charge carrier density. At the CNP, it has its maximum magnitude, but only slightly away it starts to close. The line cut at $V_g = 0.2\,\mathrm{V}$ already bears little sign of the gap Δ. We therefore conclude that it must be a feature intrinsic to the low-energy band structure of bilayer graphene and that this gap is formed spontaneously at zero magnetic and at *zero* electric field. We emphasize that the electric field induced by the back-gate voltage in the vicinity of the gap feature of $V_g \approx 100\,\mathrm{mV}$ is negligible. In the tight-binding band structure calculation of McCann [16] an induce a gap of $\Delta = 2.5\,\mathrm{mV}$, as we observe it in our experiment,

would require a back-gate voltage of at least 10 V. The Δ gap can be associated with the $\nu = 0$ state, as the low-conductance region in the color scale plot of Fig. 2b extends from large magnetic fields all the way down to zero magnetic field with no apparent phase boundary [32], distinctly different to the finding of Weitz *et al.* [18]. Although sample B1 and B2 have a $\nu = 0$ state around the CNP in our argument, these states are electrically different. In sample B1, the resistance evidently increases to infinity, whereas it stays finite in B2. This difference can be explained by insulating phases, differing in their edge-state structure [11, 13, 28].

Sample B1 has two phases, a low-magnetic field phase and a broken symmetry state induced by a small magnetic field of $B > B_{crit}$. The latter most likely is a quantum Hall ferromagnet [11, 12, 22]. The phase at low magnetic field has been assigned to a gapped anomalous Hall insulator (AHI) in which topologically protected edge states should provide a conductance of up to $4e^2/h$ [11, 13, 33]. This scenario is somewhat supported by the quantum Hall states at $\nu \pm 4$ that persist all the way down to $B = 0$ (see arrows in Fig. 2c). A similar observation has been made in compressibility measurements by Martin et al. [33]. Because B2 is the cleaner sample of the two [35], we rather think that low-field phase of B1 is a normal state, not a broken symmetry state. In contrast, the low-density phase of B2 is a broken symmetry state with edge states. If we subtract the small gap δ in sample B2, the measured conductance G is $\approx 0.8\, e^2/h$, which is smaller than the ballistic channel conductance of any gapped phase with edge states. This suggests that the gapped phase is either not single domain or that the edge states are not topologically protected, allowing for partial back-scattering. Further work is needed to determine the nature of the edge states and assign it to broken electron-hole, valley or spin-symmetry [11, 13, 36, 37].

In conclusion, using differential conductance spectroscopy we found a new type of bilayer whose spectral density is gapped at zero magnetic and zero electric field. Though this state is due to an insulating phase, the non-vanishing conductance $\approx 0.8\, e^2/h$, which is surprisingly robust in magnetic field, suggests that edge states are present.

This work was financed by the Swiss NSF, the ESF programme Eurographene, the NCCR Nano and the NCCR Quantum. We acknowledge access to Raman microscope provided by C. Stampfer and C. Hierold. We are also grateful to A. Baumgartner, D. Maslov, A. Morpurgo, A. Yacoby, V. Fal'ko and L. Levitov for discussions.

* Electronic address: Christian.Schoenenberger@unibas.ch

[1] D. C. Tsui, H. L. Stormer, and A. C. Gossard, Phys. Rev. Lett. **48**, 1559 (1982).
[2] X. Du, I. Skachko, F. Duerr, A. Luican, and E. Y. Andrei, Nature **462**, 192 (2009).
[3] K. I. Bolotin, F. Ghahari, M. D. Shulman, H. L. Stormer, and P. Kim, Nature **462**, 196 (2009).
[4] E. Wigner, Phys. Rev. **46**, 1002 (1934).
[5] S. Das Sarma, S. Adam, E. H. Hwang, and E. Rossi, Rev. Mod. Phys. **83**, 407 (2011).
[6] E. McCann and V. I. Fal'ko, Phys. Rev. Lett. **96**, 086805 (2006).
[7] K. S. Novoselov, E. McCann, S. V. Morozovi, V. I. Fal'ko, M. I. Katsnelson, U. Zettler, D. Jiang, F. Schnedin, and A. K. Geim, Nature Phys. **2**, 177 (2006).
[8] H. Min, G. Borghi, M. Polini, and A. H. MacDonald, Phys. Rev. B **77**, 041407(R) (2008).
[9] R. Nandkishore and L. Levitov, Phys. Rev. Lett. **104**, 156803 (2010).
[10] F. Zhang, H. Min, M. Polini, and A. H. MacDonald, Phys. Rev. B **81**, 041402 (2010).
[11] R. Nandkishore and L. Levitov, Phys. Rev. B **82**, 115124 (2010).
[12] E. V. Gorbar, V. P. Gusynin, and V. A. Miransky, JETP Letters, **91**, 314 (2010).
[13] F. Zhang, J. Jung, G. A. Fiete, Q. Niu, and A. H. MacDonald, Phys. Rev. Lett. **106**, 156801 (2011).
[14] J. Moser, A. Barreiro, and A. Bachtold, Appl. Phys. Lett. **91**, 163513 (2007).
[15] K. Bolotin, K. J. Sikes, Z. Jiang, M. Klima, G. Fudenberg, J. Hone, P. Kim, and H. L. Stormer, Solid State Commun. **146**, 351 (2008).
[16] E. McCann Phys. Rev. B **74**, 161403(R) (2006).
[17] J. B. Oostinga, H. B. Heersche, X. Liu, A. F. Morpurgo, and L. M. K. Vandersypen, Nature Mater. **7**, 151 (2008).
[18] R. T. Weitz, M. T. Allen, B. E. Feldman, J. Martin, and A. Yacoby, Science **330**, 812 (2010).
[19] S.-M. Choi, S.-H. Jhi, and Y.-W. Son, Nano Lett. **10**, 3486 (2010).
[20] M. Mucha-Kruczynski, I. Aleiner and V. Fal'ko, arXiv:1104.5029.
[21] B. E. Feldman, J. Martin, and A. Yacoby, Nature Phys. **5**, 889 (2009).
[22] K. Nomura and A. H. MacDonald, Phys. Rev. Lett. **96**, 256602 (2006).
[23] Y. Zhang, Z. Jiang, J. P. Small, M. S. Purewal, Y.-W. Tan, M. Fazlollahi, J. D. Chudow, J. A. Jaszczak, H. L. Stormer, and P. Kim Phys. Rev. Lett. **96**, 136806 (2006).
[24] Y. Zhao, P. Cadden-Zimansky, Z. Jiang, and P. Kim, Phys. Rev. Lett. **104**, 066801 (2010).
[25] D. A. Abanin, K. S. Novoselov, U. Zeitler, P. A. Lee, A. K. Geim, and L. S. Levitov, Phys. Rev. Lett. **98**, 196806 (2007).
[26] J. G. Checkelsky, L. Li, and N. P. Ong, Phys. Rev. B **79**, 115434 (2009).
[27] L. Zhang, Y. Zhang, M. Khodas, T. Valla, and I. A. Zaliznyak, Phys. Rev. Lett. **105** 046804 (2010).
[28] S. Raghu, X.-L. Qi, C. Honerkamp, and S.-C. Zhang, Phys. Rev. Lett. **100**, 156401 (2008).
[29] S. V. Morozov, K. S. Novoselov, M. I. Katsnelson, F. Schedin, D. C. Elias, J. A. Jaszczak, and A. K. Geim, Phys. Rev. Lett. **100**, 016602 (2008).
[30] X. Du, I. Skachko, A. Barker, and E. Y. Andrei, Nature Nanotech. **3**, 491 (2008).
[31] J. R. Williams, D. A. Abanin, L. DiCarlo, L. S. Levitov, and C. M. Marcus, Phys. Rev. B **80**, 045408 (2009).
[32] See supplementary material at

http://link.aps.org/supplemental/...
[33] J. Martin, B. E. Feldman, R. T. Weitz, M. T. Allen, and A. Yacoby, Phys. Rev. Lett. **105**, 256806 (2010).
[34] M. H. Devoret, D. Esteve, H. Grabert, G. L. Ingold, H. Pothier, and C. Urbina, Phys. Rev. Lett. **64**, 1824 (1990).
[35] We can convert B2 into B1 by exposing the sample to air. To convert B1 into B2 requires current annealing at low temperatures.
[36] D. A. Abanin, P. A. Lee, and L. S. Levitov, Phys. Rev. Lett. **96**, 176803 (2006).
[37] I. Martin, Y. M. Blanter, and A. F. Morpurgo, Phys. Rev. Lett. **100**, 036804 (2008).